

# Iodine Adsorption of Shaped Silicalite-1 Silica Zeolite

Jia Zhou<sup>1</sup>, Pu Bai<sup>1</sup>, Tianchi Li<sup>1</sup>, Qi Chen<sup>1</sup>, Tian Lan<sup>1</sup>, Fang Liu<sup>1</sup>, Zhongwei Yuan<sup>1</sup>, Weifang Zheng<sup>1</sup>, Wenfu Yan<sup>2</sup>, and Taihong Yan<sup>1</sup>

<sup>1</sup>Affiliation not available

<sup>2</sup>Jilin University

April 16, 2024

## Abstract

The effective adsorption capture of iodine produced in the spent fuel reprocessing is an effective way to avoid the harm of iodine to the ecological environment and human health. In the investigation described herein, a new kind of shaped silicalite-1 all-silica zeolite with a binder which was for direct industrial application other than power was synthesized and tested for iodine adsorption performance. Although the existence of binder in shaped silicalite-1 all-silica zeolite, it still exhibited high iodine adsorption capacities of 507 mg g<sup>-1</sup>, which was superior to inorganic adsorbents such as silver-containing zeolite mainly used currently, and was comparable with that of power silicalite-1 reported previously. Moreover, the shaped silicalite-1 all-silica zeolite could be cyclic utilization due to its reversible adsorption. All these show that the shaped silicalite-1 all-silica zeolite provides the possibility for the application of iodine adsorption in industrial post-processing condition

## Iodine Adsorption of Shaped Silicalite-1 Silica Zeolite

Jia Zhou<sup>1</sup>, Pu Bai<sup>2</sup>, Tianchi Li<sup>1</sup>, Qi Chen<sup>1</sup>, Tian Lan<sup>1</sup>, Fang Liu<sup>1</sup>, Zhongwei Yuan<sup>1</sup>, Weifang Zheng<sup>1</sup>, Wenfu Yan<sup>3\*</sup>, Taihong Yan<sup>1\*</sup>

(1. China Institute of Atomic Energy, 102413, Beijing, China 2. Luoyang Jalon Micro-Nano New Materials Co., Ltd, 471900, Luoyang, China 3. Jilin University, 130012, Changchun, China) First corresponding author : Taihong Yan, e-mail: [yanth@ciae.ac.cn](mailto:yanth@ciae.ac.cn) Second corresponding author : Wenfu Yan, e-mail: [YANW@JLU.EDU.CN](mailto:YANW@JLU.EDU.CN)

**Abstract:** Nuclear energy is one of the most promising clean energy sources in the future. The effective adsorption capture of iodine produced in the spent fuel reprocessing is an effective way to avoid the harm of iodine to the ecological environment and human health. Efforts have been made to devise materials, which can effectively capture radioactive iodine without being damaged by moisture and nitric acid. In the investigation described herein, a new kind of shaped silicalite-1 all-silica zeolite with a binder which was for direct industrial application other than power was synthesized and tested for iodine adsorption performance. Although the existence of binder in shaped silicalite-1 all-silica zeolite, it still exhibited high iodine adsorption capacities of 507 mg g<sup>-1</sup>, which was superior to inorganic adsorbents such as silver-containing zeolite mainly used currently, and was comparable with that of power silicalite-1 reported previously. Moreover, the shaped silicalite-1 all-silica zeolite could be cyclic utilization due to its reversible adsorption. All these show that the shaped silicalite-1 all-silica zeolite provides the possibility for the application of iodine adsorption in industrial post-processing conditions.

**Key words:** spent fuel reprocessing; iodine adsorption; shaped all-silica zeolite

## 1. Introduction

Nuclear energy is one of the most promising clean energy sources for mankind in the future, and spent fuel contains a large amount of raw material uranium, solid and gaseous radioactive elements produced by fission as well. During spent fuel reprocessing, processes such as shearing and dissolving, nitric acid recovery, process solution and liquid waste evaporation, waste calcination and melting, etc. will all produce process tail gas. The capture of the fission product  $^{129}\text{I}$  in the nuclear fuel cycle is a growing priority for nuclear wasteform research and development. Due to its long half-life ( $t_{1/2}$ - $1.57 \times 10^7$  year) and high mobility in most geological environments, its removal is a difficult problem.  $^{129}\text{I}$  is of concern for spent nuclear fuel reprocessing facilities and in this regard a review of  $^{129}\text{I}$  immobilization has recently been published<sup>1</sup>. Therefore, the capture and storage of gaseous iodine in off-gas has become the most important issue in the treatment of radioactive waste gas in the world<sup>2</sup>.

In the current PUREX process, radioiodine can be eliminated from the gaseous waste streams by counter-current scrubbing of the off-gas, including alkaline washing method, Mercurex method and Iodox method, etc<sup>3</sup>. But it has shortcomings such as high corrosivity, high fluidity, difficult storage, and secondary pollution<sup>3</sup>. Therefore, solid adsorption has been widely developed on iodine adsorption with the advantages of economical, convenient and highly effective. Moreover, using solid adsorbents to remove gaseous iodine can avoid the complication in system designing and high maintenance costs. The solid adsorbents mainly include activated carbon, inorganic porous materials, metal-organic frameworks, and porous organic materials. Although organic adsorption materials like metal-organic frameworks and porous organic materials have large adsorption capacity, they are not stable enough under water vapor conditions and are prone to adhesion, which are not suitable under actual working conditions. In addition, their manufacturing process is cumbersome. For these reasons, the currently promising solid adsorbents for gaseous iodine adsorption are mainly inorganic adsorbents, including activated carbon<sup>3-8</sup>, silver-loaded silica gel<sup>9-12</sup>, silver-loaded alumina<sup>13-15</sup> and silver-exchanged zeolite<sup>16-22</sup>. Among them, the silver-exchanged zeolites are most commonly used for iodine capture, being considered as a benchmark sorbent.

Domestic and foreign scholars found that zeolites with silver nitrate can capture molecular iodine and iodine alkyl compounds, with decontamination factors higher than  $10^{323-28}$ . The saturated adsorption capacity was  $196.6 \text{ mg g}^{-1}$  for elemental iodine and the average utilization rate of silver atoms was greater than 86.5%<sup>29</sup>. But one important disadvantage of Ag-based zeolites is that only a portion of silver species participate in the  $\text{I}_2$  and  $\text{CH}_3\text{I}$  capturing processes, but all of the spent solid sorbents need to be discarded after the adsorption process<sup>30</sup>. Although AgI and  $\text{AgIO}_3$  in the spent adsorbents can be converted back to  $\text{Ag}^0$  nanoparticles by the treatment with molecular hydrogen at high temperatures (ca. 773 K), the regenerated Ag nanoparticles undergo gradual sintering during the regeneration process, which leads to a significant decrease in their activity. Due to this deleterious feature, the expensive adsorbents are typically discarded after being recycled several times<sup>30</sup>. In addition, previous studies showed that the iodine adsorption performances of silver-containing zeolites were readily influenced by nitrogen oxides, which was due to the oxidation of metallic silver<sup>22,31-33</sup>. And increasing the maximum iodine adsorption capacity of the adsorbent can reduce the amount of secondary solid waste after the adsorption of radioactive iodine. There is an urgent need to find a zeolite adsorbent that is cheap, recyclable, especially suitable for industrial application.

All-silica zeolite has good hydrophobicity, acid resistance and thermal stability, which is suitable under actual spent fuel reprocessing conditions<sup>30,34,35</sup>. More importantly, it is cheap than Ag-loaded zeolite which shows a potential for iodine adsorption. Currently, the all-silica zeolites tested for iodine adsorption are poorly documented. A.Hijazi et.al studied the iodine adsorption on polyethyleneimine impregnated nanosilica sorbents. Several nanoporous silica of SBA-15 and Aerosil types were impregnated with branched polyethyleneimine with the aim to evaluate their iodine adsorption performance. The adsorption capacities of the adsorbents increased almost linearly with the N content provided by polyethyleneimine below certain threshold<sup>35</sup>. Tung Cao Thanh Pham et. al discussed power silicalite-1 all-silica zeolite on iodine adsorption performance. They observed silicalite-1 were stable in 5 M nitric acid and adsorbed iodine from highly acidic off-gas mixtures to much greater extents than does activated carbon. The iodine adsorption capacity for silicalite-1 was  $480 \text{ mg g}^{-1}$ , and after hydrophobicity intensification, it performed better up to  $530 \text{ mg g}^{-130}$ . However, in practical engineering applications, the adsorbent needs to be formed into spherical or strip-shaped materials with a

size of micrometers or millimeters through a molding process, because powder materials can not be directly used in engineering applications. In the molding process, it is generally necessary to mix inorganic binders and adsorbent powders. High-temperature calcination is performed to enhance the mechanical strength of the spherical or strip-shaped materials and ensure that no pulverization occurs under actual application conditions after preliminary molding. Generally, inorganic materials used as binders do not have gas molecule adsorption capacity, thus the maximum adsorption capacity of the adsorbent after molding is generally lower than the maximum adsorption capacity of the adsorbent powder.

In this work, a new kind of shaped silicalite-1 all-silica zeolite was synthesized by a novel method with aluminum oxide as a binder which could be directly used in industrial applications. It was strip-shaped with a diameter of 3 mm and a length of about 1cm with a topological structure of MFI molecular sieve. The adsorption properties for iodine were investigated under the condition of reprocessing temperature about 348 K subsequently <sup>36</sup>.

## 2. Experiments

### 2.1 Materials

Preparation of shaped silicalite-1 silica zeolite: A certain amount of TAPOH and silica sol were mixed and stirred at room temperature for 2 hours. The solution was moved into a stainless steel reactor lined with polytetrafluoroethylene and the reactor was placed in an oven at 423 K for 24 hours. Then the product was centrifuged, washed, and dried overnight at 353 K. The obtained powder sample was placed in a muffle furnace and calcined at 823 K for 3 hours to obtain the powdered silicalite-1. After that, the powdered silicalite-1 and pseudoboehmite were mixed evenly according to the ratio of 86:14 with water. Extruded them with an extruder and dried in an oven at 373 K. The obtained shaped sample was placed in a muffle furnace and calcined at 823 K for 2 hours to obtain the final product shaped silicalite-1. Its appearance was columnar with a diameter of 3 mm and a length of about 10 mm.

### 2.2 Iodine adsorption/desorption experiments and iodine adsorption kinetic

Both iodine adsorption and desorption experiments conducted mainly used the gravimetric method in this study. The I<sub>2</sub> capture was conducted under typical fuel reprocessing conditions (348 K and ambient pressure with an I<sub>2</sub> vapor pressure of 0.014 atm<sup>37</sup>). For each measurement, the dried adsorbent was placed in a pre-weighed glass vial. The vial and excess solid iodine were put together in a closed system at 348 K and ambient pressure. The iodine-loaded adsorbent was recovered after different exposure times and allowed to cool in an inert environment, and the mass change was recorded.

The iodine adsorption curve at 348 K was simulated for adsorption kinetics, the adsorption kinetic model was investigated and the adsorption kinetic fitting parameters were calculated.

To examine the iodine retention capacity of adsorbent, the iodine desorption experiments were evaluated. Removed the adsorbent that has adsorbed iodine out of the iodine vapor environment and leaved it open, continued to investigate iodine desorption at 398 K. The iodine-desorbed adsorbent was recovered after different exposure times and allowed to cool in an inert environment, and the mass change was recorded.

### 2.3 Characterization of adsorbents before and after iodine adsorption

The pore parameters of the adsorbents were characterized by N<sub>2</sub> adsorption/desorption isotherm at 77 K using the ASAP 2460. Powder X-ray diffraction(XRD) patterns were collected with a BRUKER D8 Advance using Cu K $\alpha$  radiation at room temperature with a step size of 0.02°, a scan time of 1 s per step, and 2 $\theta$  ranging from 5 to 70°. The generator setting was 40kV and 40 mA. Scanning electron microscopy(SEM) used JSM-7800F and energy dispersive spectroscopy(EDS) was carried out using a Tescan Vega3. X-ray Photoelectron Spectrometer(XPS) studies were performed using an Kratos AXIS Supra equipped with a monochromatic Al K $\alpha$  X-ray source.

## 3. Results and discussions

### 3.1 Characterization of adsorbents before iodine adsorption

The nitrogen adsorption/desorption isotherm and pore size distribution of the adsorbent are shown in Figure 1 and Figure 2 below. It can be seen that it basically conformed to the type-I adsorption isotherm, indicating that the pores in the adsorbent were mainly micropores. The specific surface area of the adsorbent was  $312.2 \text{ mg g}^{-1}$ , and total pore volume was  $0.27 \text{ mL g}^{-1}$ . The pore size was mainly concentrated at  $0.59 \text{ nm}$ .

Figure 1 Nitrogen adsorption-desorption isotherm measured at  $77 \text{ K}$

Figure 2 Pore size distribution of silicalite-1

### 3.2 Iodine adsorption experiments

The iodine adsorption curve of shaped silicalite-1 at  $348 \text{ K}$  is shown in Figure 3. At first 15 hours of the adsorption experiment, the amount of adsorption on shaped silicalite-1 was proportional to the adsorption time. After that, the adsorption speed slowed down, finally reached the adsorption platform after about 23 h. After the adsorption completed, the color of shaped silicalite-1 changed from white to red-brown, as shown in Figure 4. The saturated adsorption capacity for shaped silicalite-1 was  $507 \text{ mg g}^{-1}$ , between those of power silicalite-1 and hydrophobicity-intensified silicalite-1<sup>30</sup>, manifesting the molding process of shaped silicalite-1 was successful. In addition, this iodine adsorption capacity was also higher than other inorganic adsorbents reported previously, demonstrating huge application potential in iodine adsorption. The results of iodine adsorption capacity in previous studies and this work are shown in Table 1.

Figure 3 Iodine uptake curves for silicalite-1 at  $348 \text{ K}$





Figure 4 Color of (a) silicalite-1 and (b) silicalite-1 after iodine adsorption

Table 1 Comparison of iodine adsorption capacity of various inorganic adsorbents

adsorbent	Temperature/K	Iodine adsorption capacity/ $\text{mg g}^{-1}$	reference
activated carbon	348	300	38
Ag@silica gel	403	200	11
Ag@Al <sub>2</sub> O <sub>3</sub>	-	230	3
Ag@zeolite	403	196	29
Power silicalite-1	298	480	30
Power silicalite-1 (hydrophobicity-intensified)	298	530	30
Shaped silicalite-1	348	507	this work

### 3.3 Iodine adsorption kinetic

In order to further explore the kinetic performance of the adsorption process, the adsorption process curve was fitted as shown in Figure 5-6. The kinetic model constants and correlation coefficients of iodine adsorption are shown in Table 2. The results showed that the adsorption process for shaped silicalite-1 conformed to the pseudo first-order adsorption kinetic equation,  $q_t = 642.6 \times (1 - e^{-0.05t})$  ( $R^2 = 0.988$ ). The adsorption processes for shaped silicalite-1 was controlled by the diffusion steps, manifesting the adsorption rate was proportional to the difference between the equilibrium adsorption capacity and the adsorption capacity at certain time.

Figure 5 Iodine uptake curves for shaped silicalite-1 using pseudo- first-order adsorption kinetic equation

Figure 6 Iodine uptake curves for shaped silicalite-1 using pseudo-second-order adsorption kinetic equation

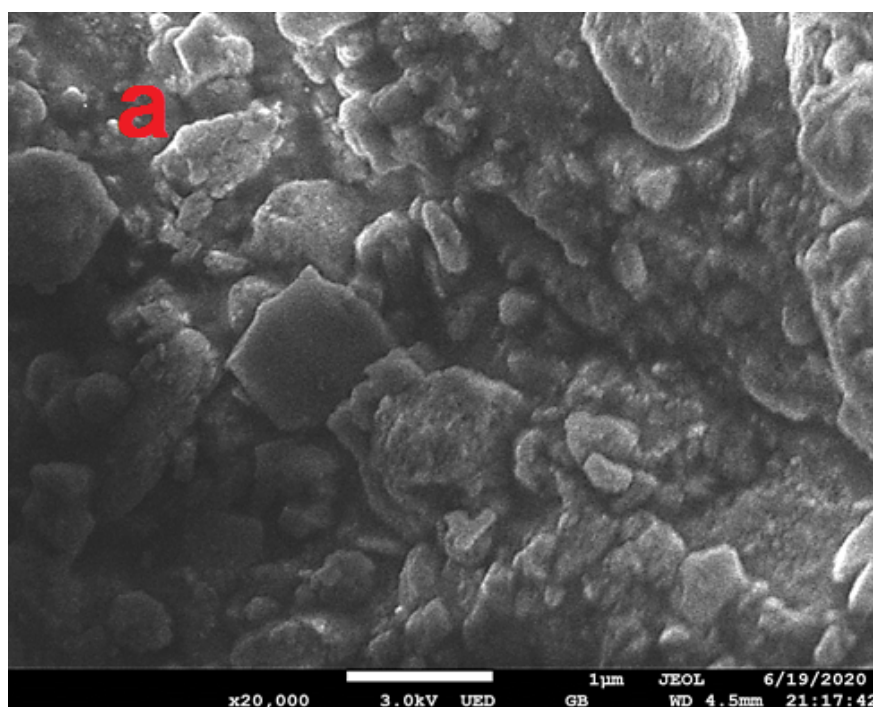
Table 2 The kinetic model constants and correlation coefficients of iodine adsorption by shaped Silicalite-1 adsorbent

Kinetics model	Kinetics model	Kinetics model			
Pseudo-first-order	Pseudo-first-order	Pseudo-first-order	Pseudo-second-order	Pseudo-second-order	Pseudo-second-order
$q_e(\text{mg/g})$	$k_1(\text{h}^{-1})$	$R^2$	$R^2$	$q_e(\text{mg/g})$	$k_2 (\text{g mg}^{-1} \text{h}^{-1})$
642.6	0.05	0.988	0.988	992.38	$3.02 \times 10^{-5}$

### 3.4 Iodine adsorption mechanism

The adsorbents before and after iodine adsorption were measured by SEM-EDS, XRD to study the iodine adsorption mechanism.

The SEM result and EDS result for shaped silicalite-1 are shown in Figure 7 and Figure 8 respectively. As the existed of the binder of aluminum oxide, the shaped silicalite-1 contained aluminum element. Although iodine did exist on shaped silicalite-1 after adsorption, no significant change in the morphology of adsorbent was observed.



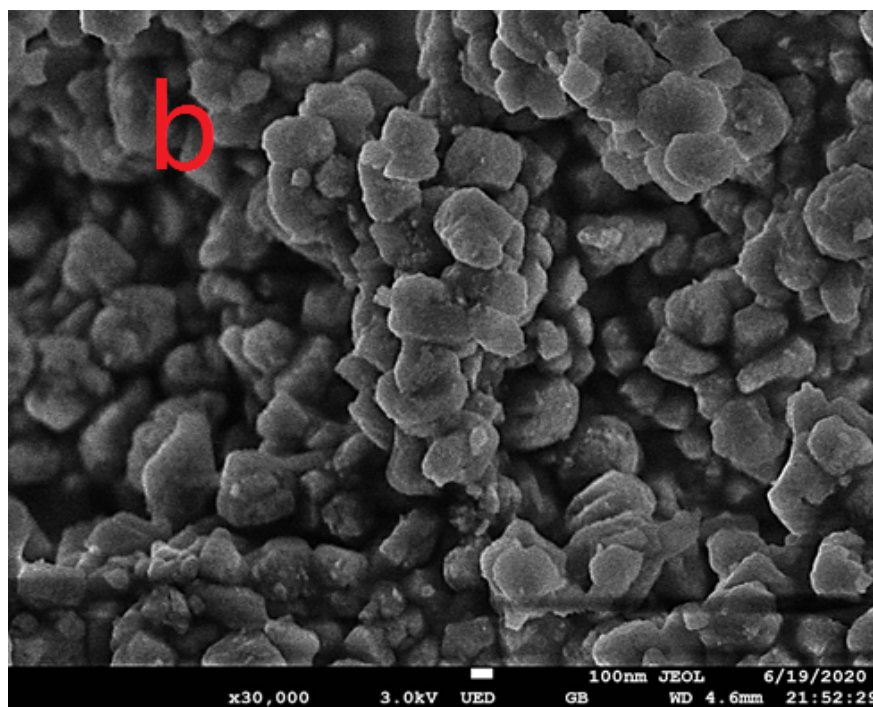
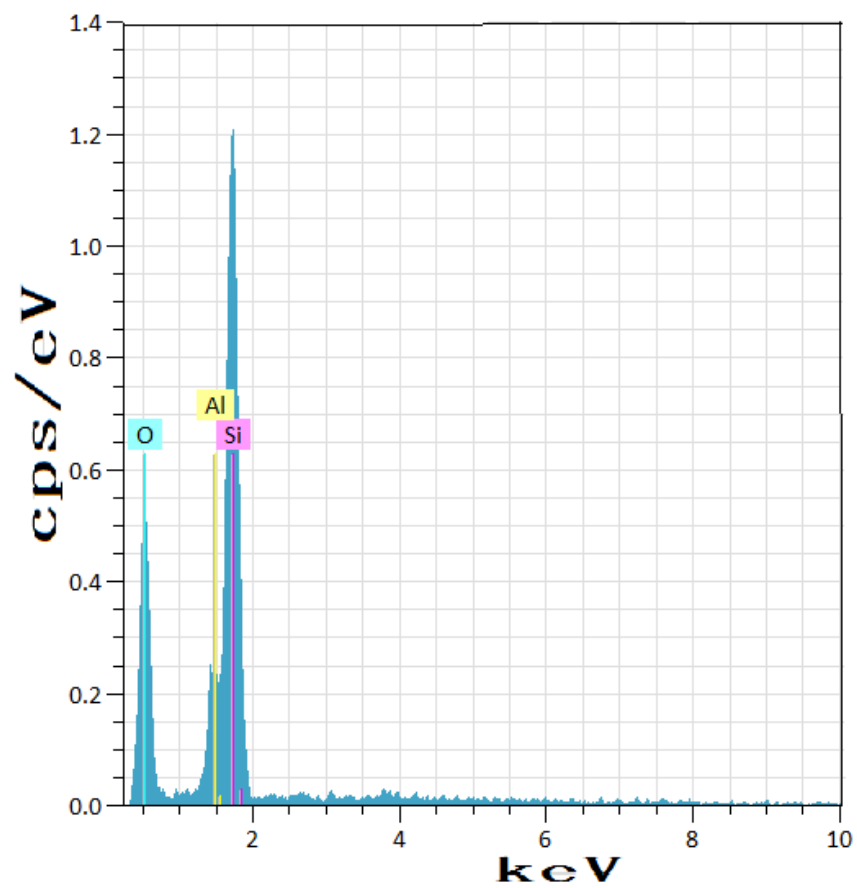
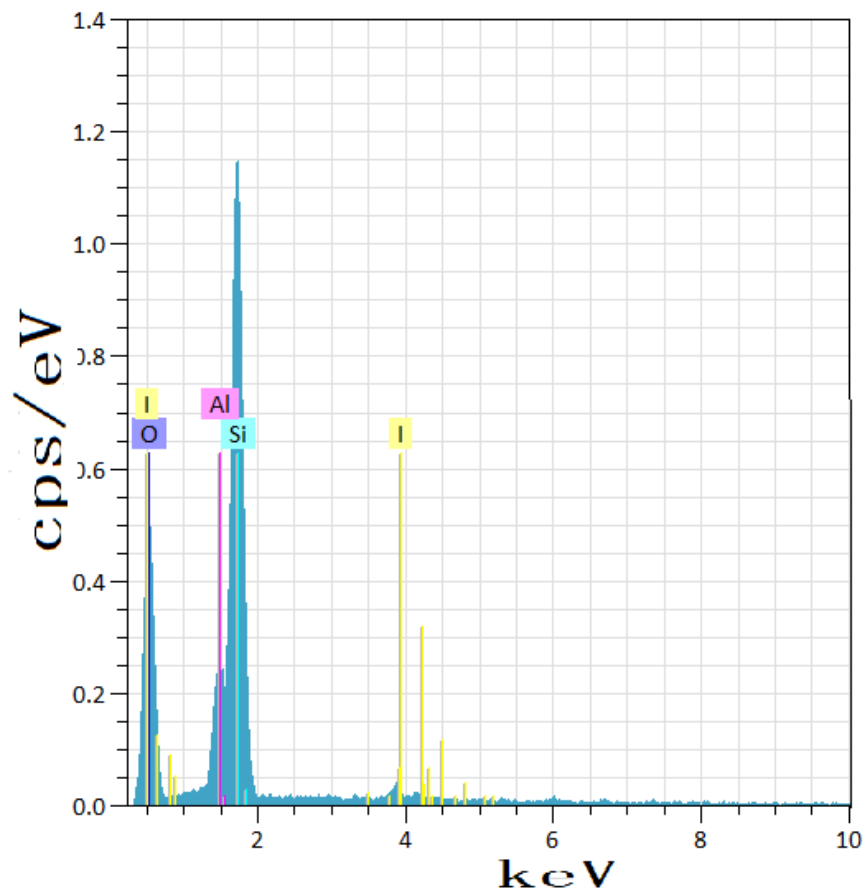


Figure7 SEM images of (a) silicalite-1 and (b) silicalite-1 after iodine adsorption



EDS spectrum of silicalite-1





(b) EDS spectrum of silicalite-1 after iodine adsorption

Figure 8 EDS Spectra of (a) silicalite-1 and (b) silicalite-1 after iodine adsorption

For studying the phase structure changes of the adsorbent after iodine adsorption, the X-ray diffraction analysis results of shaped silicalite-1 before and after iodine adsorption are shown in Figure 9. After iodine adsorption, the diffraction peaks of the two crystal planes [101] and [200] became smaller, indicating that shaped silicalite-1 adsorbed iodine and affected the long range order of the two crystal planes. It might be caused by the blocked pores of adsorbed iodine. Meanwhile, there was no new phase produced after adsorption, indicating probably that the mechanism was physical adsorption, which was proved by subsequent desorption experiment. In addition, there was no obvious diffraction peak of elemental iodine on the adsorbent after adsorption. It might be due to the elemental iodine had better dispersion on the adsorbent or the peak was weaker and annihilated, thus no obvious diffraction peak could be formed.

Figure 9 XRD patterns of silicalite-1

To investigate the existing form of iodine on the adsorbent after adsorption, the results measured by XPS are shown in Figure 10. The scan of  $I_{3d}$  showed that binding energy were 618.7eV and 630.3eV, which confirmed the iodine existed in a neutral state<sup>39</sup>.

Figure 10 XPS Spectrum of silicalite-1 after iodine adsorption

### 3.4 Iodine desorption experiments

To examine the reusable possibility of shaped silicalite-1, the iodine desorption experiments after iodine

adsorption on shaped silicalite-1 were tested at 348 K, 373 K and 398 K. The iodine desorption curves are shown in Figure 11. The EDS spectrum and XRD pattern on shaped silicalite-1 after iodine desorption are shown in Figure 12 and Figure 13 respectively. The results showed that the combination of adsorbent and iodine was reversible, and followed a physical combination. Moreover, the higher the temperature, the faster the desorption rate of iodine. Iodine adsorbed under the saturated vapor pressure of iodine at 348 K could be desorbed completely after 6 hours proved by EDS spectrum when the temperature increased at 398 K in Figure 12. Moreover, the structure of shaped silicalite-1 had no change after iodine desorption, manifesting the stability of adsorbent. It can be considered that the shaped silicalite-1 all-silica zeolite could be recycled repeatedly and continued to be used for iodine adsorption, providing the possibility for iodine removal industrial applications.

Figure 11 Iodine desorption curves for silicalite-1 at different temperatures

Figure 12 XRD patterns of silicalite-1

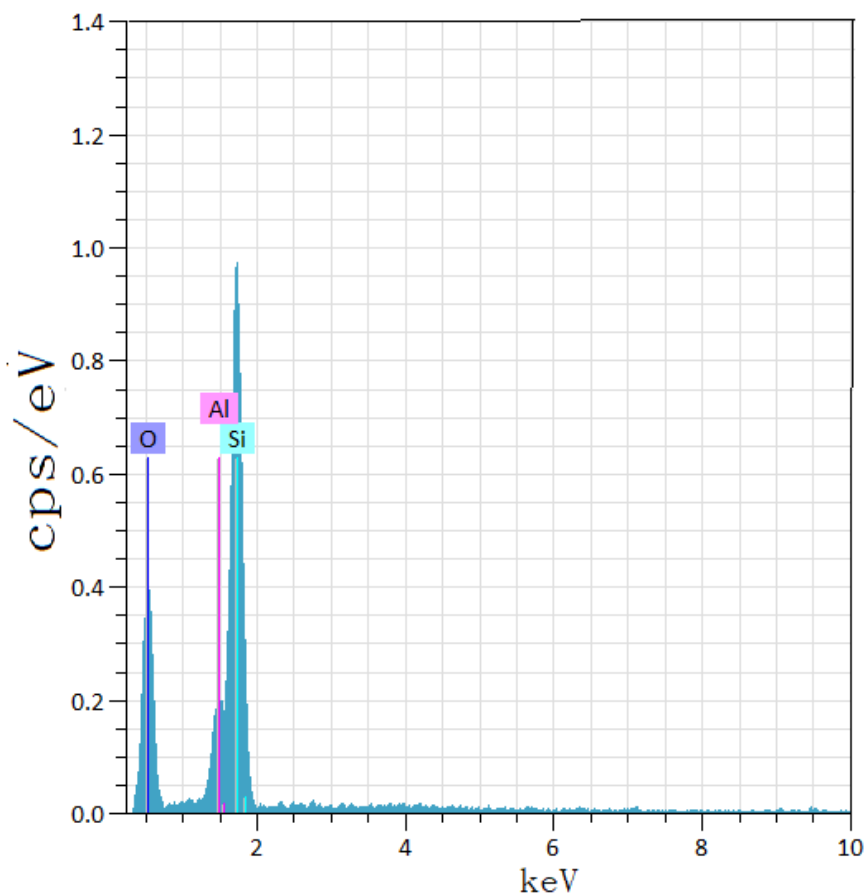


Figure 13 EDS Spectrum of shaped silicalite-1 after iodine desorption

#### 4. Conclusions

In this paper, a new kind of shaped silicalite-1 all-silica zeolite with a binder which was for directly industrial application other than power was synthesized and tested for iodine adsorption performance. Although the existence of binder in shaped silicalite-1 all-silica zeolite, it still exhibited high iodine adsorption capacities up to  $507 \text{ mg g}^{-1}$ , attributed to the appropriate micropore which had stronger adsorption potential

and hydrophobic surface. This iodine adsorption capacity was superior to inorganic adsorbents such as silver-containing zeolite mainly used currently, and was also comparable with that of power silicalite-1 reported previously, demonstrating the molding process of shaped silicalite-1 with binder was successful. The adsorption results indicated that the mechanisms of adsorption followed physical combination. Moreover, the shaped silicalite-1 all-silica zeolite could be cyclic utilization due to its reversible adsorption, and the structure of shaped silicalite-1 was still stable after iodine desorption. The static iodine adsorption capacity obtained on all-silica zeolites at the certain temperature of off-gas during spent fuel reprocessing is filling the gap which has not been reported yet at 348 K. Instead of high price of silver-containing adsorbents, this lower cost of shaped silicalite-1 all-silica zeolite which can be directly applied in industry provides the feasible path in iodine removal aspects.

## Acknowledgements

We acknowledge the financial support from the National Natural Science Foundation of China (U1967215), the 111 Project (B17020) and China National Nuclear Corporation (LC202309000903).

## Reference

1. Eric R. Vance CG, Inna Karatchevtseva, Zaynab Aly, A. Stopic, Jennifer Harrison, Gordon Thorogood, Henri Wong, Daniel J. Gregg. Immobilization of Iodine via Copper Iodide. *Journal of Nuclear Materials*. 2018;505:143-148.
2. Wang Tan XG, Shun Zhang, Yang Li, Meicheng Zhang, Xing Li, Xiaofeng Li, Lijian Ma, Shoujian Li,. Synthesis of Nitrogen-Rich Covalent Organic Framework and its Adsorption Property for Volatile Iodine. *Scientia Sinica Chimica*.2019;49(1):207-214.
3. Longqi Yue DL. Research Development of Locating Radioiodine by Solid Sorbent in a Gas Medium. *Materials Review*. 2012;26(20):285-289.
4. Minglv Ye YM, Jingjuan Tang, Shijun Lu. Study on Removal of Radioiodine from Off-Gases of Nuclear Fuel Reprocessing of Power Reactor. *Nuclear Techniques*.1985(02):65-68.
5. Longqing Yue DL, Ziyu Yue. Study of Desorption of Methyl Iodide from Activated Carbon Impregnated by TEDA. *Radiation Protection*. 2013;33(5):275-279.
6. Longqing Yue DL, Ziyu Yue. Activated Carbon Impregnated by Hexamethylene Tetramine for Localization of  $\text{CH}_3\text{I}$ . *Journal of Nuclear and Radiochemistry*.2013;35(2):121-124.
7. S. A. Kulyukhin NAK, I. A. Rumer. Sorbents for Treatment of Water Vapor–Air Flows to Remove Volatile Organic Compounds of Radioactive Iodine. *Radiochemistry*.2009;51(3):283-286.
8. Junbo Zhou YL, Liping Gao. Removal of Gaseous Iodine from Waste Gas by Using Activated Carbon Sorption. *Ship Science and Technology*. 2008;30(4):104-106.
9. S. A. Kulyukhina IAR, V. B. Krapukhina. IR Spectroscopy of the Gas Phase Formed after Interaction between  $\text{CH}_3\text{I}$  and Ag-Containing Sorbents Based on Silica Gel. *Russian Journal of Physical Chemistry A*. 2020;94(3):465-470.
10. S. A. Kulyukhin LVM, I. A. Rumer, N. A. Konovalova. Thermal Decomposition of  $\text{CH}_3^{131}\text{I}$  in a Gas Flow. *Radiochemistry*. 2013;55(4):404-409.
11. Jingjuan Tang MY, Yun Mao, Shijun Lu, Zhihua Tang, Zehong Guo. Investigation of Adsorption Properties of the Silver Nitrate Impregnated Silica Gels for Radioiodine. *Chinese Journal of Nuclear Science and Engineering*1987;7(2):144-163.
12. Josef Maty´aVs ESI, Libor KovaVr´ik. Silver-Functionalized Silica Aerogel towards an Understanding of Aging on Iodine Sorption Performance. *RSC Advances*. 2018;8:31843-31852.

13. Xin Wang TZ. Synthesis and Performance Evaluation of  $\text{AgNbO}_3/\text{Al}_2\text{O}_3$  High-Temperature-Resistant Adsorbent for Radioiodine. *Journal of Nuclear and Radiochemistry*. 2018;40(4):250-257.
14. Jae Hwan Yang H-SP, Yung-Zun Cho.  $\text{Al}_2\text{O}_3$  Containing Silver Phosphate Glasses as Hosting Matrices for Radioactive Iodine. *Journal of Nuclear Science and Technology*. 2017;54(12):1330-1337.
15. Andrew Miller YW. Al-O-F Materials as Novel Adsorbents for Gaseous Radioiodine Capture. *Journal of Environmental Radioactivity*. 2014;133:35-39.
16. Bruno Azambre MC, Amal Hijazi, . Effects of the Cation and Si/Al Ratio on  $\text{CH}_3\text{I}$  Adsorption by Faujasite Zeolites. *Chemical Engineering Journal*. 2020;379:122308.
17. Alexander I. Wiechert APL, Jisue Moon, Carter W. Abney, Yue Nan, Seungrag Choi, Jiuxu Liu, Lawrence L. Tavlarides, Costas Tsouris, Sotira Yiacoumi. Capture of Iodine from Nuclear-Fuel-Reprocessing Off-Gas : Influence of Aging on a Reduced Silver Mordenite Adsorbent after Exposure to  $\text{NO}/\text{NO}_2$ . *Applied Materials & Interfaces*. 2020.
18. R. T. Jubin JAJ, S. H. Bruffey. *Extended Elemental Iodine Adsorption by AgZ under Prototypical Vessel Off-Gas Conditions* : Oak Ridge National Laboratory;2018.
19. Yue Nan LLT, David W. DePaoli. Adsorption of Iodine on Hydrogen-Reduced Silver-Exchanged Mordenite: Experiments and Modeling. *AIChE Journal*. 2017;63(3):1024-1035.
20. Tomáš BuVcko SC, Jean-Francois Paul, Laurent Cantrel, Michael Badawi. Dissociative Iodomethane Adsorption on Ag-MOR and Formation of AgI Clusters an Ab-Initio Molecular Dynamics Study 2017:1-14, Physical Chemistry Chemical Physics.
21. Carter W. Abney YN, Lawrence L. Tavlarides. X-ray Absorption Spectroscopy Investigation of Iodine Capture by Silver-Exchanged Mordenite. *Industrial & Engineering Chemistry Research*. 2017;56:4837-4846.
22. S. H. Bruffey KKP, J. F. Walker Jr., R. T. Jubin. *Complete NO and NO<sub>2</sub> Aging Study for AgZ* : Oak Ridge National Laboratory;2015.
23. S. A. Kulyukhin LVM, N. A. Konovalova, I. A. Rumer, E. V. Zanina. Localization of  $\text{CH}_3^{131}\text{I}$  from Water Vapor–Air Flow on Granulated Sorbents Containing Nanoparticles of Ag and Ni Compounds. *Radiochemistry*. 2015;57(3):266-272.
24. Qinghui Cheng WY, Zejun Li, Qiufeng Zhu, Taiwei Chu, Dehua He, Chao Fang Adsorption of Gaseous Radioactive Iodine by Ag13X Zeolite at High Temperatures. *Journal of Radioanal Nuclear Chemistry*. 2015;303:1883-1889.
25. Tina M. Nenoff MAR, Nick R. Soelberg, Karena W. Chapman. Silver-Mordenite for Radiologic Gas Capture from Complex Streams: Dual Catalytic  $\text{CH}_3\text{I}$  Decomposition and I Confinement. *Microporous and Mesoporous Materials*. 2014;200:293-303.
26. Karena W. Chapman PJC, Tina M. Nenoff. Radioactive Iodine Capture in Silver-Containing Mordenites through Nanoscale Silver Iodide Formation. *Journal of American Chemical Society*. 2010;132:8897-8899.
27. N B Mikheev ANK, S A Kulyukhin, I A Rumer, V L Novichenko. Sorption of  $\text{CH}_3^{131}\text{I}$  from Steam-Gas Phase on Modified Ag-Containing Zeolites. *Radiochemistry*. 2001;43(4):405-408.
28. Byung Seon Choi GIP, Joon Hyung Kim. Adsorption Equilibrium and Dynamics of Methyl Iodide in a Silver Ion-Exchanged Zeolite Column at High Temperatures. *Adsorption*. 2001;7:91-103.
29. Minglv Ye JT, Ding Xu, Zhiming He, Zhihua Tang. A Study of the Adsorption Properties of the Silver Nitrate Impregnated Mordenite for Airborne Radioiodine. *Journal of Nuclear and Radiochemistry*. 1991;13(3):169-175.

- 30.** Tung Cao Thanh Pham SD, In Chul Hwang, Mee Kyung Song, Do Young Choi, Dohyun Moon, Peter Oleynikov, Kyung Byung Yoon. Capture of Iodine and Organic Iodides Using Silica Zeolites and the Semiconductor Behaviour of Iodine in a Silica Zeolite. *Energy & Environmental Science*. 2016;9(3):1050-1062.
- 31.** S.H. Bruffey RTJ, K.K. Anderson, J.F. Walker, Jr. *Aging of Iodine-Loaded Silver Mordenite in NO<sub>2</sub>* : Oak Ridge National Laboratory;2014.
- 32.** K.K. Patton SHB, R.T. Jubin, J.F. Walker, Jr. *Iodine Loading of NO Aged Silver Exchanged Mordenite* : Oak Ridge National Laboratory;2014.
- 33.** K P Kaara SHB, R T Jubin. Effects of Extended In-Process Aging of Silver - Exchanged Mordenite on Iodine Capture Performance. Paper presented at: Proceedings of the 33rd Nuclear Air Cleaning Conference2014; St Louis,MO.
- 34.** Jae Hwan Yang YJC, Jin Myeong Shin , Man Sung Yim. Bismuth-Embedded SBA-15 Mesoporous Silica for Radioactive Iodine Capture and Stable Storage. *Journal of Nuclear Materials*. 2015;465:556-564.
- 35.** A. Hijazi BA, G. Finqueneisel, F. Vibert, J.L. Blin. High Iodine Adsorption by Polyethyleneimine Impregnated Nanosilica. *Microporous and Mesoporous Materials*. 2019.
- 36.** Chan Yao HL, Guowen Su, Huiwen Li, Jin Bai, Tingting Li, Yanhong Xu. Synthesis of Porous Organic Materials and Their Use in Iodine Adsorption. *Journal of Jilin Normal University(Natural Science Edition)*. 2018;39(3):27-31.
- 37.** Karena W. Chapman DFS, Gregory J. Halder, Peter J. Chupas, Tina M. Nenoff. Trapping Guests within a Nanoporous Metal Organic Framework through Pressure-Induced Amorphization. *Journal of American Chemical Society*.2011;133:18583-18585.
- 38.** Hui Ma J-JC, Liangxiao Tan, Jian-Hua Bu, Yanhong Zhu, Bien Tan, Chun Zhang. Nitrogen-Rich Triptycene-Based Porous Polymer for Gas Storage and Iodine Enrichment. *ACS Macro Letters*. 2016(9).
- 39.** Wen Yuan Pei JY, Hui Wu, Wei Zhou, Yingwei Yang, Jianfang Ma,. A Calix Resorcinarene-Based Giant Coordination Cage: Controlled Assembly and Iodine Uptake. *Chemical Communications*. 2020;56(16):2491-2494.